Inverse Scattering Method for One-Dimensional Inhomogeneous Lossy Medium by Using a Microwave Networking Technique

Tie Jun Cui and Chang Hong Liang

Abstract— **The formulation of reflection coefficients from an inhomogeneous lossy medium illuminated by TE and TM waves is approximately derived, in closed form, by using a microwave network method. From the formulation, a novel inverse scattering scheme to reconstruct simultaneously the permittivity and conductivity profiles, is proposed. This scheme is suitable for both continuous and discontinuous profiles, under both the weak scattering and strong scattering conditions. It has also been shown that when the conductivity of the medium equals zero, the reconstructed result of this scheme will reduce to the one in [14]. Numerical and closed-form reconstruction examples show the validity of the scheme.**

I. Introduction

FOR THE reconstruction of one-dimensional inhomogeneous lossy medium, many authors have investigated various methods [1]-[13]. These methods may be generally classified into two approaches. The first approach is inverse mapping. Generalization or modification of Gel'fand–Levitan type equation is representative of this approach. The best fitting method or the iterative procedure is the second approach. This approach is usually formulated by the source-type integral equation which related the constitutive parameter of the medium to the scattering field.

In this paper, we will investigate the inverse scattering problem by using a microwave networking technique. From the viewpoint of the microwave network, we first derive the reflection coefficients of an inhomogeneous lossy medium illuminated by TE and TM waves approximately in closed forms, from which a novel inverse scattering scheme to reconstruct simultaneously the permittivity profile and the conductivity profile is proposed, also in closed form. This scheme can be used for both continuous and discontinuous media. It has been shown that the reconstructed result of the scheme will reduce to the one in reference [14] when the conductivity of the medium equals zero. A remarkable instance of the novel scheme with the published closed-form approximations is that the scheme is not only suitable for weak-scattering condition, but also suitable for strong-scattering condition. Reconstruction examples show the applicability of the scheme.

Manuscript received February 11, 1993; revised April 24, 1995.

The authors are with the Department of Electromagnetic Field Engineering, Xidian University, Xi'an, 710071, P. R. China.

IEEE Log Number 9412664.

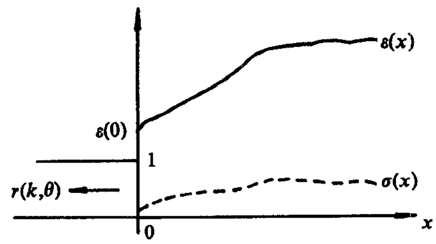

Fig. 1. A half-space inhomogeneous lossy medium.

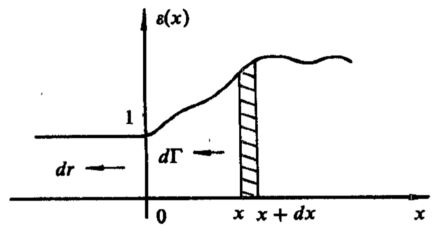

Fig. 2. The lossy medium whose permittivity profile is continuous at the interface $x = 0$.

II. Derivation of the Reflection Coefficients

We consider a half-space inhomogeneous lossy medium shown in Fig. 1. A time harmonic electromagnetic plane wave (TE polarized or TM polarized) of wave number k is incident from the left free space upon the medium at an oblique angle θ. The permittivity relative to free space and the conductivity are functions of the geometric distance x. $r(k, \theta)$ represents the frequency-domain reflection coefficient of the medium.

To obtain the reflection coefficient, we discuss the following three stages.

A. The Permittivity Profile is Continuous in the Whole Space

In this case, the medium is illustrated in Fig. 2.

For an arbitrary point $x(x \geq 0)$ in the x-axis, the complex relative permittivity of the lossy medium is

$$\tilde{\epsilon}(x) = \epsilon(x) - j\frac{\sigma(x)}{\omega\epsilon_0} = \epsilon(x) - j\frac{\eta_0\sigma(x)}{k} \tag{1}$$

where $\eta_0 = \sqrt{\mu_0/\epsilon_0} = 120\pi\Omega$ is the wave impedance of the free space.

Make a differential increment dx, and suppose that the relative permittivities and the conductivities at points x and $x + dx$ are $\epsilon(x)$, $\epsilon(x) + d\epsilon(x)$, $\sigma(x)$ and $\sigma(x) + d\sigma(x)$, respectively.

From the electromagnetic wave theory [15] and the classical idea of Bremmer [16], [17], the Fresnel differential-reflection coefficients caused by the region $[x, x + dx]$ are

$$d\Gamma^{\perp} = \frac{n(x) - n(x+dx)}{n(x) + n(x+dx)} \tag{2}$$

$$d\Gamma^{\|} = \frac{\tilde{\epsilon}(x+dx)n(x) - \tilde{\epsilon}(x)n(x+dx)}{\tilde{\epsilon}(x+dx)n(x) + \tilde{\epsilon}(x)n(x+dx)} \tag{3}$$

which correspond to TE polarized wave and TM polarized wave, respectively, where $n(x) = \sqrt{\tilde{\epsilon}(x) - \sin^2\theta}$.

To derive the reflection coefficients at the interface, we consider the transmission coefficients for TE wave and TM wave of the thin layer between x and $x + dx$. In first approximation, these coefficients are given by

$$dT^{\perp}_{\rightarrow}\, exp\left[-jkn(x)dx\right] \tag{4}$$

$$dT^{\|}_{\rightarrow}\, exp\left[-jkn(x)dx\right] \tag{5}$$

where

$$dT^{\perp}_{\rightarrow} = \frac{2n(x)}{n(x) + n(x+dx)} = \left[1 + \frac{dn(x)}{2n(x)}\right]^{-1} \tag{6}$$

$$\begin{aligned} dT^{\|}_{\rightarrow} &= \frac{2n(x)\sqrt{\tilde{\epsilon}(x)\tilde{\epsilon}(x+dx)}}{n(x)\tilde{\epsilon}(x+dx) + n(x+dx)\tilde{\epsilon}(x)} \\ &= \left\{1 + \frac{d[n(x)\tilde{\epsilon}(x)]}{2n(x)\tilde{\epsilon}(x)}\right\}^{-1} \end{aligned} \tag{7}$$

in which

$$dn(x) = [n(x+dx) - n(x)] + O(dx^2), \; \cdots. \tag{8}$$

Since (4) and (5) are only accurate up to $O(dx)$, it is convenient to write (6) and (7) in the forms that are more suitable for repeated multiplication

$$dT^{\perp}_{\rightarrow} = \exp\left\{-\frac{1}{2}\frac{dn(x)}{n(x)}\right\} + O(dx^2) \tag{9}$$

$$dT^{\|}_{\rightarrow} = \exp\left\{-\frac{1}{2}\frac{d[n(x)\tilde{\epsilon}(x)]}{n(x)\tilde{\epsilon}(x)}\right\} + O(dx^2). \tag{10}$$

Carrying out the multiplication for all layers in the region $[0, x]$ then leads to the first order WKB transmission coefficients from 0 to x in a continuous medium

$$T^{\perp}_{\rightarrow} = \exp\left\{-\frac{1}{2}\int_0^x \frac{dn(x')}{n(x')}\right\} \exp\left[-jk\int_0^x n(x')\,dx\right] \tag{11}$$

$$T^{\|}_{\rightarrow} = \exp\left\{-\frac{1}{2}\int_0^x \frac{d[n(x')\tilde{\epsilon}(x')]}{n(x')\tilde{\epsilon}(x')}\right\} \exp\left[-jk\int_0^x n(x')\,dx'\right]. \tag{12}$$

In the meantime, the transmission coefficients for TE wave and TM wave of the thin layer from $x + dx$ to x are similarly derived

$$dT^{\perp}_{\leftarrow} = \exp\left\{\frac{1}{2}\frac{dn(x)}{n(x)}\right\} + O(dx^2) \tag{13}$$

$$dT^{\|}_{\leftarrow} = \exp\left\{\frac{1}{2}\frac{d[n(x)\tilde{\epsilon}(x)]}{n(x)\tilde{\epsilon}(x)}\right\} + O(dx^2) \tag{14}$$

which give the first order WKB solutions from x to 0 as

$$T^{\perp}_{\leftarrow} = \exp\left\{\frac{1}{2}\int_0^x \frac{dn(x')}{n(x')}\right\} \exp\left[-jk\int_0^x n(x')\,dx'\right] \tag{15}$$

$$T^{\|}_{\leftarrow} = \exp\left\{\frac{1}{2}\int_0^x \frac{d[n(x')\tilde{\epsilon}(x')]}{n(x')\tilde{\epsilon}(x')}\right\} \exp\left[-jk\int_0^x n(x')\,dx'\right]. \tag{16}$$

Hereby the differential reflection coefficients of the medium at $x = 0$ caused by the thin layer between x and $x + dx$ are obtained by neglecting the high order infinitesimal

$$dr^{\perp} = T^{\perp}_{\rightarrow} d\Gamma^{\perp} T^{\perp}_{\leftarrow} = d\Gamma^{\perp} \exp\left[-j2k\int_0^x n(x')\,dx'\right] \tag{17}$$

$$dr^{\|} = T^{\|}_{\rightarrow} d\Gamma^{\|} T^{\|}_{\leftarrow} = d\Gamma^{\|} \exp\left[-j2k\int_0^x n(x')\,dx'\right] \tag{18}$$

which can be rewritten as a common form

$$dr = d\Gamma \exp\left[-j2k\int_0^x n(x')\,dx'\right]. \tag{19}$$

Since the permittivity profile is continuous at the interface of free space with the medium, the total reflection coefficient of the medium in frequency domain can be written as

$$r(k, \theta) = \int_0^{+\infty} \frac{d\Gamma}{dx} \exp\left[-j2k\int_0^x n(x')\,dx'\right] dx. \tag{20}$$

Under a high frequency and low-loss approximation

$$\frac{\eta_0\sigma(x)}{k[\epsilon(x) - \sin^2\theta] \ll 1} \tag{21}$$

we have

$$n(x) \approx \sqrt{\epsilon(x) - \sin^2\theta} - j\frac{\eta_0\sigma(x)}{2k\sqrt{\epsilon(x) - \sin^2\theta}}. \tag{22}$$

Then (2) and (3) turn to

$$d\Gamma^{\perp} \approx -\frac{d\epsilon(x)}{4[\epsilon(x) - \sin^2\theta]} \tag{23}$$

$$d\Gamma^{\|} \approx \frac{[\epsilon(x) - 2\sin^2\theta]d\epsilon(x)}{4\epsilon(x)[\epsilon(x) - \sin^2\theta]} \tag{24}$$

and the reflection coefficient (20) turns

$$r(k, \theta) = \int_0^{+\infty} \frac{d\Gamma}{dx} \exp\left[-\alpha(x)\right] \exp\left[-j2ky(x)\right] dx \tag{25}$$

where

$$\alpha(x) = \int_0^x \frac{\eta_0\sigma(x')}{\sqrt{\epsilon(x') - \sin^2\theta}}\, dx' \tag{26}$$

$$y(x) = \int_0^x \sqrt{\epsilon(x') - \sin^2\theta}\, dx'. \tag{27}$$

Let

$$t = 2y(x) = 2\int_0^x \sqrt{\epsilon(x') - \sin^2\theta}\, dx' \tag{28}$$

then (25) is converted into

$$r(k, \theta) = \int_0^{+\infty} \frac{1}{2\sqrt{\epsilon(x) - \sin^2\theta}} \frac{d\Gamma}{dx} \exp[-\alpha(x)] e^{-jkt}\, dt \tag{29}$$

by the definition of the Fourier transform, the inverse Fourier transform of $r(k, \theta)$ is directly achieved from (29)

$$R(t, \theta) = \frac{\exp[-\alpha(x)]}{2\sqrt{\epsilon(x) - \sin^2\theta}} \frac{d\Gamma}{dx} \tag{30}$$

where the relation between t and x is shown in (28). Considering (23) and (24), we have

$$R^{\perp}(t, \theta) = -\frac{\exp[-\alpha(x)]}{8[\epsilon(x) - \sin^2\theta]^{3/2}} \frac{d\epsilon(x)}{dx} \tag{31}$$

$$R^{\parallel}(t, \theta) = -\frac{[\epsilon(x) - 2\sin^2\theta]\exp[-\alpha(x)]}{8\epsilon(x)[\epsilon(x) - \sin^2\theta]^{3/2}} \frac{d\epsilon(x)}{dx} \tag{32}$$

which are the inverse Fourier transforms of the reflection coefficients of the medium shown in Fig. 2, illuminated by TE wave and TM wave, respectively.

B. The Permittivity Profile has a Discontinuity at the Interface $x = 0$

Fig. 1 shows an example of this type medium. From Fig. 1, the permittivity profile has a discontinuity at the interface $x = 0$, i.e., $\epsilon(0) \neq 1$. By the viewpoint of microwave network, this discontinuity is equivalent to a microwave transmission line junction, whose equivalent network is shown in Fig. 3(a)

In Fig. 3(a), the parameters in the frame are the S scattering matrix of the network; $r_0(k, \theta)$ represents the reflection coefficient of a continuous lossy medium shown in Fig. 3(b). In detail, under the high-frequency and low loss approximation (22)

$$R_{01}^{\perp} = \frac{\cos\theta - \sqrt{\epsilon(0) - \sin^2\theta}}{\cos\theta + \sqrt{\epsilon(0) - \sin^2\theta}} \tag{33}$$

$$R_{01}^{\parallel} = \frac{\epsilon(0)\cos\theta - \sqrt{\epsilon(0) - \sin^2\theta}}{\epsilon(0)\cos\theta + \sqrt{\epsilon(0) - \sin^2\theta}} \tag{34}$$

which corresponds to TE wave and TM wave, respectively.

According to the microwave network theory, we obtain from Fig. 3(a)

$$r(k, \theta) = R_{01} + \frac{(1 - R_{01}^2) r_0(k, \theta)}{1 + R_{01} r_0(k, \theta)}. \tag{35}$$

Thus

$$r_0(k, \theta) = \frac{r(k, \theta) - R_{01}}{1 - R_{01} r(k, \theta)}. \tag{36}$$

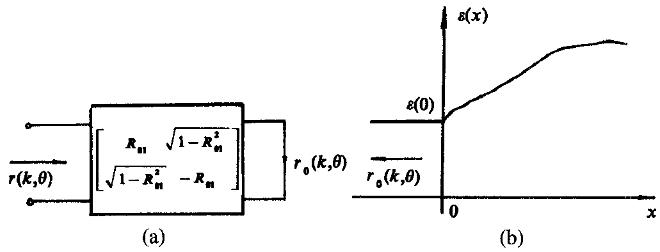

Fig. 3. The equivalent transmission line junction network of the permittivity profile discontinuity and a continuous lossy medium whose permittivity profile is continuous at the interface $x = 0$.

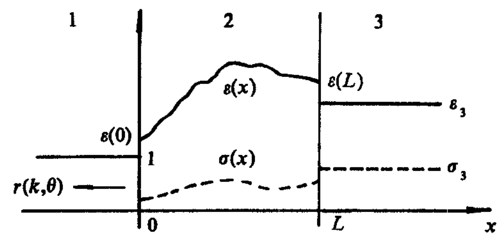

Fig. 4. A discontinuous lossy medium whose permittivity profile has two discontinuities at $x = 0$ and $x = L$.

On the other hand, $r_0(k, \theta)$ is the reflection coefficient of the continuous medium shown in Fig. 3(b) whose permittivity profile is continuous at the interface $x = 0$. So from the similar derivation to Case A, we can directly write out

$$R_0^{\perp}(t, \theta) = -\frac{\exp[-\alpha(x)]}{8[\epsilon(x) - \sin^2\theta]^{3/2}} \frac{d\epsilon(x)}{dx} \tag{37}$$

$$R_0^{\parallel}(t, \theta) = -\frac{[\epsilon(x) - 2\sin^2\theta]\exp[-\alpha(x)]}{8\epsilon(x)[\epsilon(x) - \sin^2\theta]^{3/2}} \frac{d\epsilon(x)}{dx} \tag{38}$$

where $R_0^{\perp}(t, \theta)$ and $R_0^{\parallel}(t, \theta)$ are the inverse Fourier transforms of $r_0^{\perp}(k, \theta)$, respectively.

In fact, when $\epsilon(0) = 1$ then $R_{01} = 0$, further $r_0(k, \theta) = r(k, \theta)$. Thus (37) and (38) reduce to (31) and (32). That is to say, (37) and (38) are the general forms of reflection coefficients.

C. The Permittivity Profile has Two Discontinuities at the Interfaces $x = 0$ and $x = L$

We consider a general case. The permittivity profile has two discontinuities at the interfaces $x = 0$ and $x = L$, as shown in Fig. 4. In this case, the medium can be equivalent to two microwave transmission line junctions cascaded with a microwave network, as shown in Fig. 5. Here, the first junction network is the same as that in Fig. 3(a). The second is the equivalent network of the second discontinuity at $x = L$, and

$$R_{12}^{\perp} = \frac{\sqrt{\epsilon(L) - \sin^2\theta} - \sqrt{\epsilon_3 - \sin^2\theta}}{\sqrt{\epsilon(L) - \sin^2\theta} + \sqrt{\epsilon_3 - \sin^2\theta}} \tag{39}$$

$$R_{12}^{\parallel} = \frac{\epsilon_3\sqrt{\epsilon(L) - \sin^2\theta} - \epsilon(L)\sqrt{\epsilon_3 - \sin^2\theta}}{\epsilon_3\sqrt{\epsilon(L) - \sin^2\theta} + \epsilon(L)\sqrt{\epsilon_3 - \sin^2\theta}} \tag{40}$$

corresponding to TE wave and TM wave, respectively.

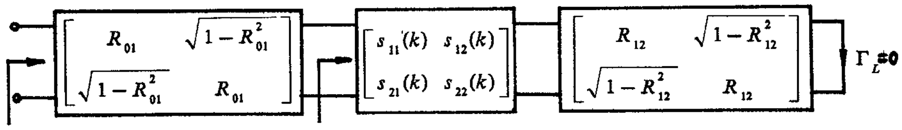

Fig. 5. The equivalent microwave network of the discontinuous lossy medium.

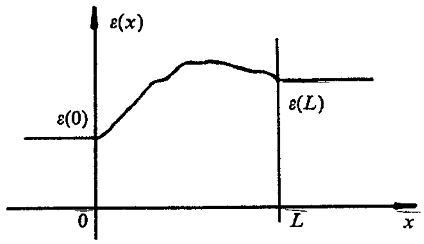

Fig. 6. A continuous lossy medium.

In Fig. 5, $s_{ij}(k)$ represents the S scattering parameter of the network which describes the continuous permittivity profile shown in Fig. 6. Through the microwave network theory, $s_{11}(k)$ is just the reflection coefficient of the continuous medium shown in Fig. 6 when the electromagnetic wave is incident from the left to the right. So carrying out the discussion in Case A, we have

$$s_{11}(k) = \int_0^L \frac{d\Gamma}{dx} \exp[-\alpha(x)] \exp[-j2ky(x)]\, dx \tag{41}$$

where $\frac{d\Gamma}{dx} = 0$ when $x > L$ has been considered.

Similarly, $s_{22}(k)$ is the reflection coefficient of the continuous medium when the electromagnetic wave is incident from the right to the left. Hereby

$$s_{22}(k) = -\int_0^L \frac{d\Gamma}{dx} \exp\{-[\alpha(L) - \alpha(x)]\} \cdot \exp\{-j2k[y(L) - y(x)]\}\, dx \tag{42}$$

where $\alpha(L)$ and $y(L)$ are expressed by (26) and (27) when $x = L$. Substituting (23) and (24) into (41) and (42) yields the expressions of $s_{11}(k)$ and $s_{22}(k)$ for TE wave and TM wave, respectively.

On the other hand, $s_{21}(k)$ represents the transmission coefficient of the continuous medium from $x = 0$ to $x = L$, so we obtain from (11) and (12)

$$s_{21}^{\perp} = \exp\left\{-\frac{1}{2} ln \frac{n(L)}{n(0)}\right\} \exp\left[-jk \int_0^L n(x')\, dx'\right] \tag{43}$$

$$s_{21}^{\parallel} = \exp\left\{-\frac{1}{2} ln \frac{n(L)\tilde{\epsilon}(L)}{n(0)\tilde{\epsilon}(0)}\right\} \exp\left[-jk \int_0^L n(x')\, dx'\right]. \tag{44}$$

Similarly, from (15) and (16), we have

$$s_{12}^{\perp} = \exp\left\{\frac{1}{2} ln \frac{n(L)}{n(0)}\right\} \exp\left[-jk \int_0^L n(x')\, dx'\right] \tag{45}$$

$$s_{12}^{\parallel} = \exp\left\{\frac{1}{2} ln \frac{n(L)\tilde{\epsilon}(L)}{n(0)\tilde{\epsilon}(0)}\right\} \exp\left[-jk \int_0^L n(x')\, dx'\right]. \tag{46}$$

Therefore, the multiplication

$$s_{12}^{\perp} s_{21}^{\perp} = s_{12}^{\parallel} s_{21}^{\parallel} = \exp\left[-j2k \int_0^L n(x')\, dx'\right]. \tag{47}$$

Under the high frequency and low loss approximation, (22), the above equation can be written as

$$s_{12}(k)s_{21}(k) = \exp[\alpha(L)] \exp[-j2ky(L)] \tag{48}$$

which is suitable for both TE wave and TM wave.

Through the microwave network theory, we obtain from Fig. 5

$$r_0(k, \theta) = s_{11}(k) + \frac{R_{12}s_{12}(k)s_{21}(k)}{1 - R_{12}s_{22}(k)} \tag{49}$$

$$r(k, \theta) = \frac{R_{01} + r_0(k, \theta)}{1 + R_{01}r_0(k, \theta)} \tag{50}$$

which are the reflection coefficients of the general medium. To derive the inverse Fourier transform of $r_0(k, \theta)$, we rewrite (49) as

$$r_0(k, \theta) = s_{11}(k) + R_{12}s_{12}(k)s_{21}(k) \cdot [1 + R_{12}s_{22}(k) + R_{12}^2 s_{22}^2(k) + \cdots]. \tag{51}$$

Taking the inverse Fourier transform of the above equation, and considering the expression (48), we have

$$R_0(t, \theta) = S_{11}(t) + R_{12} \exp[-\alpha(L)]\{\delta(t) + R_{12}S_{22}(t) + R_{12}^2 S_{22}^2(t) * S_{22}^2(t) + \cdots\} * \delta(t - T) \tag{52}$$

where $R_0(t, \theta)$, $S_{11}(t)$ and $S_{22}(t)$ are the inverse Fourier transforms of $r_0(k, \theta)$, $s_{11}(k)$ and $s_{22}(k)$, where $\exp[-\alpha(L)]\delta(t - T)$ is the inverse Fourier transform of $s_{12}(k)s_{21}(k)$, where $\delta(t)$ is Dirac-δ function, "$*$" represents convolution, and where

$$T = 2y(L) = 2\int_0^L \sqrt{\epsilon(x) - \sin^2\theta}\, dx. \tag{53}$$

Through the convolution theory $f(t) * \delta(t - T) = f(t - T)$, we infer from (52)

$$R_0(t, \theta) = S_{11}(t) \text{ when } 0 \le t \le T. \tag{54}$$

Considering (41), yield

$$S_{11}(t) = \frac{\exp[-\alpha(x)]}{2\sqrt{\epsilon(x) - \sin^2\theta}} \frac{d\Gamma}{dx} \tag{55}$$

which gives

$$R_0^{\perp}(t, \theta) = -\frac{\exp[-\alpha(x)]}{8[\epsilon(x) - \sin^2\theta]^{3/2}} \frac{d\epsilon(x)}{dx} \tag{56}$$

$$R_0^{\parallel}(t, \theta) = -\frac{[\epsilon(x) - 2\sin^2\theta]\exp[-\alpha(x)]}{8\epsilon(x)[\epsilon(x) - \sin^2\theta]^{3/2}} \frac{d\epsilon(x)}{dx} \tag{57}$$

when $0 \le t \le T$.

III. Reconstruction of the Lossy Medium

A. Reconstruction of the Permittivity Profile

In the inhomogeneous lossy medium shown in Fig. 1, if the conductivity profile is known, we will reconstruct the permittivity profile by using either the reflection coefficient of TE incident wave or TM incident wave. We select the former. From (37), we have

$$R_0^{\perp}(t, \theta)\exp[\alpha(x)]dt = -\frac{d\epsilon(x)}{4[\epsilon(x) - \sin^2\theta]} \tag{58}$$

where (28) is considered. Integrating the above equation, yields

$$\epsilon(x) = \sin^2\theta + [\epsilon(0) - \sin^2\theta] \cdot \exp\left\{-4\int_0^t R_0^{\perp}(t', \theta)\exp[\alpha(x')]\, dt'\right\} \tag{59}$$

which is the reconstruction formula of the permittivity profile, where t and $\alpha(x)$ are expressed as (28) and (26), respectively.

When the permittivity profile of the lossy medium has a discontinuity at $x = L$, the inverse Fourier transforms of the reflection coefficients are of the same forms as (37) and (38) in the region $0 \le t \le T$, as shown in (56) and (57). So the inversion formula (59) is also suitable for the discontinuous medium.

From the form of (59) we will note that it is a coupling equation, because the right term of the equation contains the unknown function $\epsilon(x)$. But in fact all the used $\epsilon(x')$ in the right term satisfy $x' \le x$, which have been reconstructed.

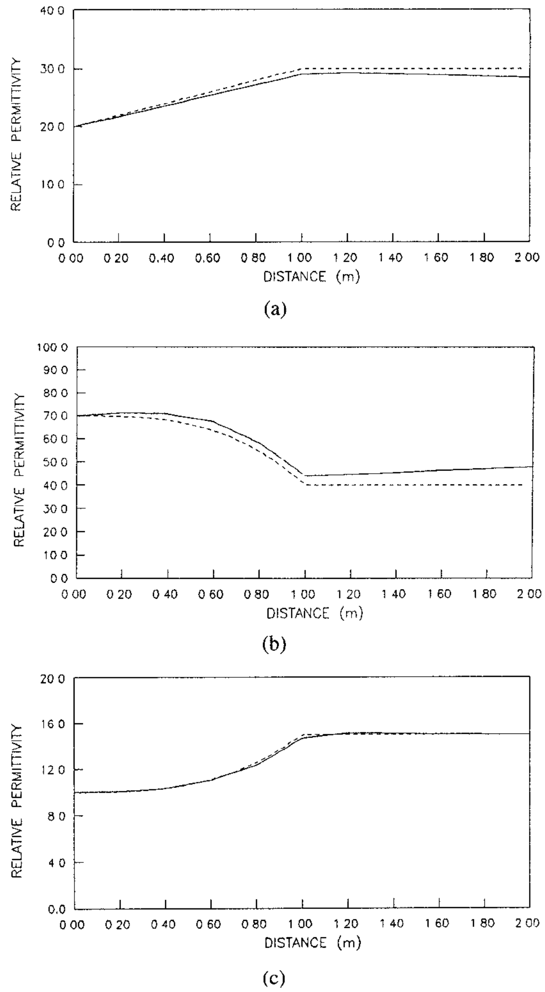

Fig. 7. Reconstruction results (solid lines) and their comparisons with exact profiles (dashed lines). (a) $n = 1$, $\eta_0\sigma(x) = 0.1$, (b) $n = 2$, $\eta_0\sigma(x) = 0.1$, (c) $n = 3$, $\eta_0\sigma(x) = 0.1$.

Thus, so long as $\epsilon(0)$ is known, $\epsilon(x)$ will be completely reconstructed.

We cite a special case. When $\theta = 0°$ and $\sigma(x) = 0$, (59) will reduce to

$$\epsilon(x) = \epsilon(0)\exp\left[-4\int_0^t R_0^{\perp}(t')\, dt'\right]. \tag{60}$$

Furthermore, when $\epsilon(0) = 1$, then $R_{01} = 0$, and $R_0^{\perp}(t) = R^{\perp}(t)$, the above equation turns

$$\epsilon(x) = \exp\left[-4\int_0^t R^{\perp}(t')\, dt'\right] \tag{61}$$

which is just the reconstruction formula in reference [14].

B. Reconstruction of both the Permittivity and Conductivity Profiles

For the inhomogeneous lossy medium, if the permittivity and conductivity profiles are simultaneously reconstructed, both reflection coefficients of TE incident wave the TM incident wave are used. From (37) and (38), we obtain

$$\epsilon(x) = \frac{2\sin^2\theta R_0^{\perp}(t, \theta)}{R_0^{\perp}(t, \theta) + R_0^{\parallel}(t, \theta)} \tag{62}$$

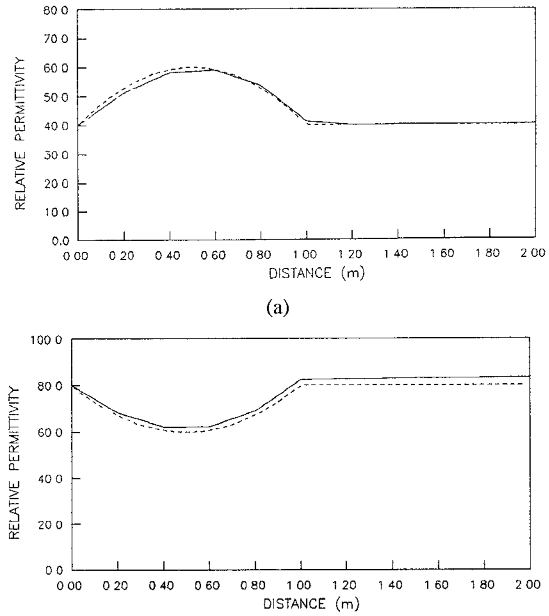

Fig. 8. Reconstruction results (solid lines) and their comparisons with exact profiles (dashed lines). (a) $\eta_0\sigma(x) = 0.1$, (b) $\eta_0\sigma(x) = 0.2$.

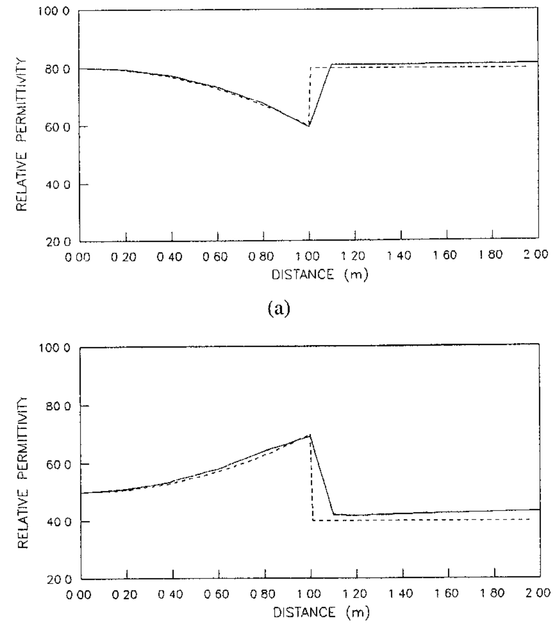

Fig. 9. Reconstruction results of discontinuous lossy medium (solid lines) and their comparison with exact profiles (dashed lines). (a) $\eta_0\sigma(x) = 0.1$, (b) $\eta_0\sigma(x) = 0.1$.

$$\exp[-\alpha(x)] = -8R_0^{\perp}(t, \theta)[\epsilon(x) - \sin^2\theta]^{3/2} / \left[\frac{d\epsilon(x)}{dx}\right]. \quad (63)$$

Considering (26), we have

$$\eta_0\sigma(x) = -\sqrt{\epsilon(x) - \sin^2\theta}\frac{d}{dx} \cdot\left\{ln\left|R_0^{\perp}(t, \theta)[\epsilon(x) - \sin^2\theta]^{3/2} / \left[\frac{d\epsilon(x)}{dx}\right]\right|\right\} \quad (64)$$

where, the relationship between t and x is also shown in (28).

Similarly, the inversion formulas (62) and (64) are also suitable for the discontinuous lossy medium.

C. Reconstruction of the Permittivity at the Interface

In the reconstruction formulas (59), (60), (62), and (64), the right terms contain $\epsilon(0)$ directly or implicitly. Therefore, if $\epsilon(x)$ and $\sigma(x)$ are completely reconstructed, $\epsilon(0)$ should be inverted first.

For a lossless medium, Hopcraft and Smith [18] have presented a method to reconstruct $\epsilon(0)$. We extended the method to the lossy case in [19].

It has been shown that, in the high frequency region, plotting the real and imaginary parts of the reflection coefficients of the lossy medium shown in Fig. 4 as a function of the wave number k yields a circle. From the intercept a and the radius b of the circle, the permittivity at the interface, $\epsilon(0)$ can be reconstructed. When the incident wave is TE polarized, the inversion formula is [19]

$$\epsilon(0) = \sin^2\theta + \cos^2\theta\left(\frac{1-q}{1+q}\right)^2 \quad (65)$$

where

$$q = \frac{1}{2a}[(b^2 - a^2 - 1) + \sqrt{(b^2 - a^2 - 1)^2 - 4a^2}] \quad (66)$$

which is suitable for both continuous profile and discontinuous profile.

IV. Reconstruction Examples

In this section, several examples are used to demonstrate the inverse scattering scheme. In these examples, the left spaces of the reconstructed media are all free space.

First, we consider the reconstruction of the permittivity profile by using (59). The reflection data are simulated by a numerical method from the exact profiles

$$\epsilon(x) = \epsilon_1 + (\epsilon_2 - \epsilon_1)\left(\frac{x}{L}\right)^n, \quad 0 \le x \le L \quad (67)$$

and the inverse Fourier transforms are obtained by FFT program. When we set $n = 1$, 2, and 3, the reconstructed results are shown in Fig. 7. Here, the medium is divided into 100 parts to compute the reflection coefficients numerically, and the wave number is chosen as $k \in [0, 10]$. In the FFT program, we set $N = 1024$. Fig. 7 also gives the exact profiles for comparisons.

From Fig. 7, our reconstruction results are accurate in any case, including the case of strong scattering. However, Fig. 7 only gives the reconstructions of monotonous profiles. Next, we consider a general case where the reflection coefficients used for reconstruction are simulated by numerical method from the exact profile

$$\epsilon(x) = Ax^2 + Bx + C. \quad (68)$$

When the parameters A, B, and C are chosen as different values, the reconstructed profiles and exact profiles are shown in Fig. 8.

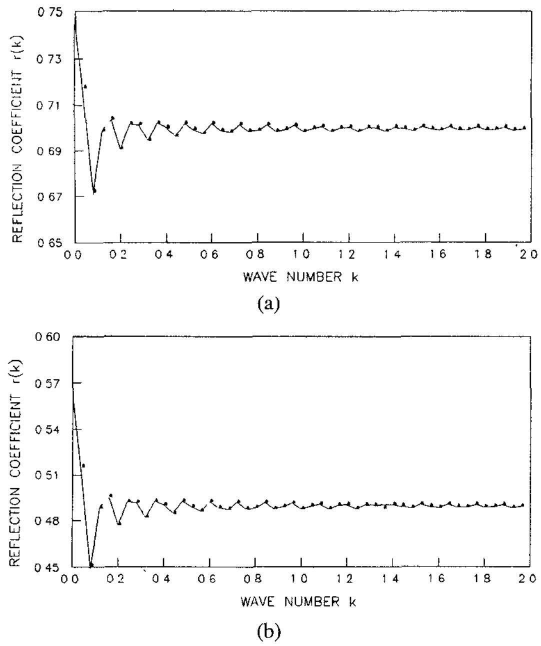

Fig. 10. The calculated reflection data (solid lines) and the given reflection data (dotted lines). (a) TE wave, (b) TM wave.

From Fig. 8, the reconstruction results are accurate no matter when the permittivity profile has a maximum or a minimum, as demonstrated in Fig. 8.

Both examples above are concerned for continuous profiles. If the permittivity profile has a discontinuity at $x = L$, the reconstruction results from (59) are displayed in Fig. 9.

From Fig. 9, the reconstructed profiles are also accurate compared with the given exact profiles in any case. That is to say, the inversion formula (59) is suitable for both continuous profile and discontinuous profile under the weak scattering condition and strong scattering condition.

Next, we consider the simultaneous reconstruction of permittivity and conductivity profiles by using (62) and (64). In this case, both the reflection coefficients of TE wave and TM wave should be used. To show the availability of the two inversion formulas, we first consider an artificial closed form example.

Suppose the reflection coefficients of an unknown lossy medium are expressed as

$$r^{\perp(\parallel)}(k,\,\theta) = \frac{\beta^{\perp(\parallel)} + I^{\perp(\parallel)}}{1 = \beta^{\perp(\parallel)} I^{\perp(\parallel)}} \tag{69}$$

where $\perp$ and $\parallel$ represent TE polarized and TM polarized, respectively. And

$$\beta^{\perp} = \frac{\cos\theta - a^2}{\cos\theta + a^2} \tag{70}$$

$$\beta^{\parallel} = \frac{(a^4 + \sin^2\theta)\cos\theta - a^2}{(a^4 + \sin^2\theta)\cos\theta + a^2} \tag{71}$$

$$I^{\perp} = -\int_0^L \frac{x\exp(-\alpha x)}{x^2 + a^2}\exp\left[-j\frac{2}{3}kx(x^2 + 3a^2)\right]dx \tag{72}$$

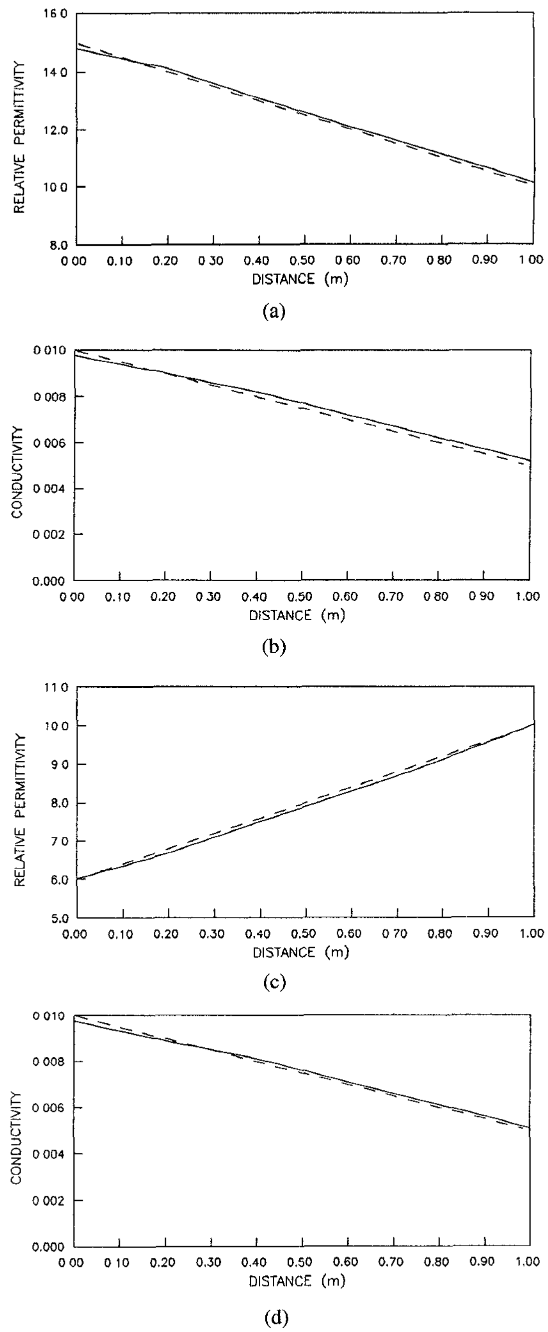

Fig. 11. Reconstruction results (solid lines) and their comparisons with exact profiles (dashed lines) when $n = 1$. (a) Permittivity, (b) conductivity, (c) permittivity, and (d) conductivity.

$$I^{\parallel} = \int_0^L \frac{(x^2 + a^2)^2 - \sin^2\theta}{(x^2 + a^2)^2 + \sin^2\theta}\,\frac{x\exp(-\alpha x)}{x^2 + a^2} \cdot\exp\left[-j\frac{2}{3}kx(x^2 + 3a^2)\right]dx \tag{73}$$

where $a > 0$, $L > 0$, $\alpha > 0$, they are all constants. Through (66) and (65), we obtain

$$\epsilon(0) = a^4 + \sin^2\theta. \tag{74}$$

Substituting it into (36) yields

$$r_0^{\perp}(k,\,\theta) = I^{\perp}, \quad r_0^{\parallel}(k,\,\theta) = I^{\parallel}. \tag{75}$$

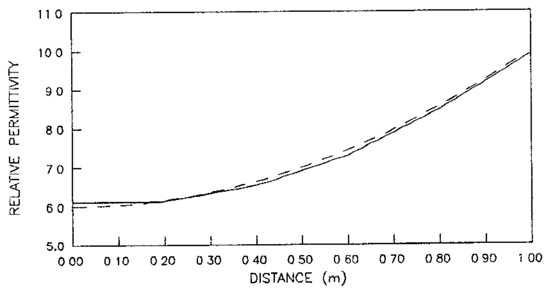

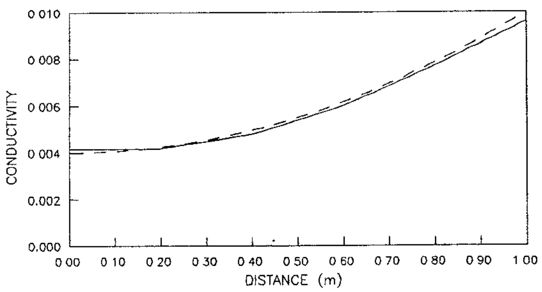

Fig. 12. Reconstruction results (solid lines) and their comparisons with exact profiles (dashed lines) when $n = 2$. (a) Permittivity, (b) conductivity.

Using a variable transformation, we obtain from (72) and (73)

$$R_0^{\perp}(t, \theta) = -\frac{x \exp(-\alpha x)^2}{2(x^2 + a^2)} \quad (76)$$

$$R_0^{\|}(t, \theta) = \frac{(x^2 + a^2)^2 - \sin^2\theta}{(x^2 + a^2)^2 + \sin^2\theta} \frac{x \exp(-\alpha x)}{2(x^2 + a^2)^2} \quad (77)$$

in which

$$t = \frac{2}{3} x(x^2 + 3a^2). \quad (78)$$

Substituting (76) and (77) into (62) and (64), we can derive

$$\epsilon(x) = (x^2 + a^2)^2 + \sin^2\theta \quad (79)$$

$$\eta_0 \sigma(x) = \alpha(x^2 + a^2) \quad (80)$$

which are the permittivity and conductivity profiles corresponding to the reflection coefficients (69). When $a = 3$, $\alpha = 0.2$, $L = 1$ and $\theta = 45°$, we calculate the reflection coefficients from the profiles given in (79) and (80) by using a numerical method. The calculated reflection data and the given reflection data by (69) to (72) are displayed in Fig. 10, which fit very well. This artificial example shows that the inversion formulas (62) and (64) are correct.

To show the applicability of the above formulas, we consider a numerical example. The reflection coefficients used for reconstruction are simulated from the following exact profiles

$$\epsilon(x) = \epsilon_1 + (\epsilon_2 - \epsilon_1)\left(\frac{x}{L}\right)^n, \qquad \sigma(x) = \sigma_1 + (\sigma_2 - \sigma_1)\left(\frac{x}{L}\right)^n. \quad (81)$$

When $n = 1$ and 2, the reconstructed profiles are displayed in Figs. 11 and 12, where we set $\theta = 60°$, $k \in [0, 10]$.

From Figs. 11 and 12, the reconstructed profiles are much accurate compared with the exact profiles when the loss is low. As the loss of the medium equals zero, the inversion formulas are also true.

V. Conclusion

In this paper, we proposed a novel inverse scattering scheme to reconstruct the permittivity profile and the conductivity profile of an inhomogeneous lossy medium by using a microwave networking technique. This scheme is suitable for both continuous and discontinuous profiles. Reconstruction examples show that the novel scheme is accurate, even if strong scattering conditions are satisfied.

Acknowledgment

The authors would like to thank the reviewers for their useful comments and suggestions.

References

[1] W. M. Boerner, A. K. Jordan, and I. W. Kay, Eds., "Special issue on inverse scattering method in electromagnetics," *IEEE Trans. Antennas Propagat.*, vol. AP-29, no. 2, Mar. 1981.
[2] V. H. Weston, "On the inverse program for a hyperbolic dispersive partial differential equations," *J. Math. Phys.*, vol. 13, pp. 1952–1956, 1972.
[3] R. J. Krueger, "An inverse program for a dissipative hyperbolic equation with discontinuous coefficients," *Q. Appl. Math.*, vol. 34, pp. 129–148, 1976.
[4] ——, "Numerical aspects of a dissipative inverse problem," *IEEE Trans. Antennas Propagat.*, vol. AP-29, no. 2, pp. 253–261, Mar. 1981.
[5] R. S. Beezley and R. J. Krueger, "An electromagnetic inverse problem for dispersive media," *J. Math. Phys.*, vol. 26, pp. 317–325, 1985.
[6] M. Mostafavi and R. Mitra, "Remote proving of inhomogeneous media using parameter optimization techniques," *Radio Sci.*, no. 2, pp. 1105–1111, Dec. 1972.
[7] A. G. Tijhuis, "Iterative determinations of permittivity and conductivity profiles of a dielectric slab in the time domain," *IEEE Trans. Antennas. Propagat.*, vol. AP-29, no. 2, pp. 239–245, Mar. 1981.
[8] T. Uno and S. Adachi, "Inverse scattering method for one-dimensional inhomogeneous layered media," *IEEE Trans. Antennas Propagat.*, vol. AP-35, pp. 1456–1466, Dec. 1987.
[9] A. G. Tijhuis, "Born-type reconstruction of material parameters of an inhomogeneous lossy dielectric slab from reflected-field data," *Wave Motion*, vol. 11, pp. 151–173, 1989.
[10] D. B. Ge and L. J. Chen, "A direct profile inversion for weakly conducting layered medium," *IEEE Trans. Antennas Propagat.*, vol. 39, pp. 907–909, July 1991.
[11] W. Tabbara, "Reconstruction of permittivity profiles from a spectral analysis of the reflection coefficient," *IEEE Trans. Antennas Propagat.*, vol. AP-27, pp. 241–244, 1979.
[12] A. G. Tijhuis, *Electromagnetic Inverse Profiling: Theory and Numerical Implementation.* Utrecht, The Netherlands: VNU Science Press, 1987, pp. 366–375.
[13] Y. Kim, N. Cho, and D. L. Jarggard, "Time-domain inverse scattering using a nonlinear renormalization technique," *JEWA*, vol. 5, pp. 99–111, 1990.
[14] H. D. Ladouceur and A. K. Jordan, "Renormalization of an inverse scattering theory for inhomogeneous dielectrics," *J. Opt. Soc. Am. A*, vol. 2, pp. 1916–1921, Nov. 1985.
[15] J. A. Kong, *Electromagnetic Wave Theory.* New York: Wiley, 1986.
[16] H. Bremmer, "The WKB approximation as the first term of a geometric-optical series," *Commun. Pure Appl. Math.*, vol. 4, pp. 105–110, 1951.
[17] F. W. Sluijter, "Generalizations of the Bremmer series based on physical concepts," *J. Math. Anal. Appl.*, vol. 27, pp. 282–302, 1969.
[18] K. I. Hopcraft and P. R. Smith, "Geometrical properties of backscattered radiation and their relation to inverse scattering," *J. Opt. Soc. Am. A*, vol. 6, pp. 508–516, Apr. 1989.
[19] T. J. Cui and C. H. Liang, "Nonlinear differential equation for the reflection coefficient of an inhomogeneous lossy medium and its inverse scattering solutions," *IEEE Trans. Antennas Propagat.*, vol. 42, no. 5, pp. 621–626, May 1994.

Tie Jun Cui was born on September 8, 1965, in Hebei, People's Republic of China. He received the B.Sc., M.Sc., and Ph.D. degrees in electrical engineering from Xidian University, Xi'an, P. R. China, in 1987, 1990, and 1993, respectively,

He joined the Department of Microwave Telecommunication Engineering, Xidian University, in March 1993. He became an Associate Professor in Nov. 1993, conducting research in electromagnetic scattering and inverse scattering, microwave network theory and data processing, and numerical methods.

In June of this year, Dr. Cui was awarded a Research Fellowship from the Alexander von Humboldt Foundation. He will become a Research Fellow with Institut fur Hochstfrequenztechnik und Electronik, Universitat Karlsruhe, Karlsruhe, Germany, engaging research in electromagnetic scattering and inverse scattering.

Chang Hong Liang was born in Shanghai, People's Republic of China, in December 1943. He graduated from the Department of Radio Physics, Northwest Telecommunication Engineering Institute in 1965.

Since 1967 he has been with the Department of Electromagnetic Engineering at the same university, where he is now a Professor, director of doctors. From 1980 to 1982 he was a Visiting Scholar in the Syracuse University, New York. He is President of Xidian University. His current research interests are computational electromagnetics, computational microwave, network theory, electromagnetic scattering and inverse scattering, electromagnetic soliton, and electromagnetic missiles.

Dr. Liang is a fellow of China Institute of Electronics (CIE) and the Vice President of Microwave Society, CIE.